Hybrid of Moment Method and Mode Matching Technique for Full-Wave Analysis of SIW Circuits

R. Rezaiesarlak, M. Salehi, and E. Mehrshahi

Department of Electrical and Computer Engineering
Shahid Beheshti University, G.C., Tehran, Iran
rezaiesarlak@gmail.com , m_salehi@sbu.ac.ir, mehr@sbu.ac.ir

Abstract ─ In this paper, a full wave analysis of substrate integrated waveguide (SIW) structures is presented based on the moment method in combination with the mode matching technique. Initially, input and output post pairs are terminated with two waveguide sections. Then waveguide width, as an unknown variable, is adjusted to obtain minimum reflection from the SIW. Field distribution in the structure and current density on posts as well as dispersion characteristic of the SIW are investigated. Also, by taking the advantage of the moment method, analysis of the structures with longitudinal discontinuity along the wave propagation direction is offered. Furthermore, versatile instances are analyzed and compared with experimental values, results from high frequency structure simulator (HFSS), and numerical methods in recent literature. Good agreement between the results verifies the accuracy of the hybrid method.

Index Terms ─ Bandpass filter, method of moment, mode expansion, mode matching technique, substrate integrated waveguide.

I. INTRODUCTION

Substrate integrated waveguides (SIW's) have emerged as a promising substitution for circuits and components operating in a millimeter-wave and terahertz region. They combine the high-Q-factor and low-loss merits of traditional rectangular waveguides with the simplicity of planar fabrication and low-cost integration. Nowadays, many microwave circuits are designed based on SIW technology [1-4]. Some empirical equations have been reported to accurately characterize the dispersion behavior of the SIW [5-7]. However, they are not accurate for all values of lateral cylinder spacing and cylinder diameter as well as frequency of operation. In [8], measurement results confirm the frequency dependence of equivalent width which has not been taken into account in closed-form formulas of [5-7].

Various numerical techniques such as finite element method (FEM), finite difference time or frequency domain (FDTD/FDFD), transmission line method (TLM), method of line (MoL), and method of moment (MoM), can be developed to analyze the structure under consideration [9-13]. Furthermore, in [14] a fast and simple technique is employed to calculate dispersion characteristics of SIW structure. However, it is not as accurate as mentioned time-consuming numerical methods for a wide range of structure parameters.

In these methods, for achieving reasonable accuracy, one must choose a grid size small enough which results in an enormous number of cells for the cavity and microstrip space and thus requires a large amount of computer memory and computation time. To overcome these problems, the hybrid of moment method and mode matching technique is employed to expand modes in the structure based on Cartesian eigenfunctions [15]. The most considerable advantage of the proposed method is that it can be easily extended to the structures with longitudinal discontinuities.

This paper is organized as follows: In section II, the theoretical issues are explained to extract the equivalent waveguide width of the SIW. Then, the extension of the proposed method to SIW

structures with longitudinal discontinuities is presented. In section III, the accuracy and generality of the proposed method is verified by a number of examples consisting of planar discontinuities in SIW structure. Finally, section V concludes the paper.

II. THEORETICAL ISSUES

A. Equivalent waveguide width of the SIW

Figure 1 shows an *x-z* cut of a typical two-port substrate integrated waveguide in which metallic posts are inserted in dielectric substrate. In order to expand the fields inside the structure based on Cartesian coordinate system, a closed metallic contour is generated to enclose the circuit as shown in Fig. 1. This enclosure consists of input and output waveguide sections with the same width of W_1 and two metallic walls far from the metallic posts. The effect of the enclosure is negligible if the field is well confined in the analyzed SIW. It is worth mentioning that the value of W_1 which causes minimum reflection at the input and output ports represents the equivalent width of the SIW. In matched condition, there is no reflection from input and output ports of the whole structure. Therefore, the equivalent width only depends on characteristic dimensions of the SIW. First, consider a pair of circular posts in the rectangular waveguide as illustrated in Fig. 2a. The equivalent problem is created by replacing the posts with a number of uniform current filaments running from top to bottom. In this case, as Fig. 2b shows, the electric Green's function of the structure can be obtained by considering a current filament at (x_i , z_i) as below

$$J_i (x_i , z_i) = I_i \delta(x - x_i) \cdot \delta(z - z_i) .$$

Afterwards, the electric field in the structure can be obtained as

$$E(x , z) = \sum_i G(x , z / x_i , z_i) I_i (x_i , z_i) .$$

By nullifying the total electric field on the post surfaces, the currents on the posts and scattering parameters of the structure are calculated [16]. In the following, the analysis of one pair of posts is generalized to multi pairs. The structure in Fig. 1 is divided into *M+2* regions. There are (*M-1*) pairs of posts instead of only one pair of posts. In fact, analysis method of one pair posts in rectangular

waveguide is firstly discussed and then is generalized to multi-posts. For the structure under consideration, as illustrated in Fig. 3a, the following current delta functions are inserted along the waveguide to obtain the Green's function of the structure.

$$I_i = \{ I_i^{(1)} , \dots , I_i^{(j)} , \dots , I_i^{(M)} \} \hat{a}_y .$$

In SIW structures only TE_{n0} modes can be excited and extracted, due to evanescence of the surface current on lateral walls. Therefore, the current filaments have no variations in *y*-direction, and hence, are uniform. The above current functions are shown in Fig. 3b. Each current filament in region k (R^k) can be described by

$$J_i^k (x_i^k , z_i^k) = I_i^k \delta(x - x_i^k) \cdot \delta(z - z_i^k) \tag{1}$$
$$i = 1, \dots , p^k .$$
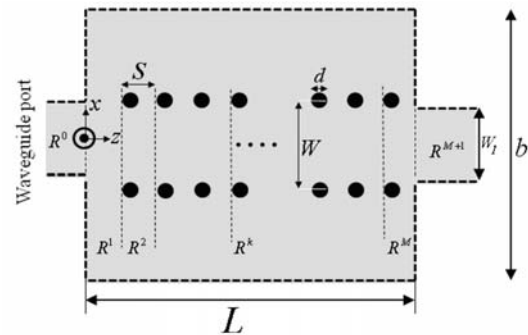
Fig. 1. Top view of the substrate integrated waveguide circuit.

In which (x_i^k , z_i^k) is the location of ith-filament in k^{th}-region and P^k is the number of current filaments in k^{th}-region. To obtain the current distribution on posts, the method of moment is employed. The scalar potential function in the region k (R^k) can be written as

$$\varphi^k = \sum \overbrace{[A_n^k exp(-j \beta z) + B_n^k exp(-j \beta z)]}^{h_n^k(z)} \times cos(\frac{n \pi(x +b / 2)}{b}) \tag{2a}$$

Similarly, the scalar potential functions for the input and output waveguide sections, as shown in Fig. 1, can be represented by

$$\varphi^0 = \sum_{n=1} B_n^0 exp(j \beta_n^* z) \times cos(\frac{n\pi(x + W_1 /2)}{W_1}) . \tag{2b}$$

$$\varphi^{M+1} = \sum_{n=1} A_n^{M+1} exp(-j\beta_n^* z) \times cos(\frac{n\pi(x + W_1 /2)}{W_1}) . \tag{2c}$$

in which A_n^k and B_n^k are coefficients of forward and reflected TE_{n0} modes in k^{th} region of Fig. 3b and

$$\beta_n = \sqrt{\omega^2\mu\varepsilon - (n\pi/b)^2} ,$$

$$\beta_n^* = \sqrt{\omega^2\mu\varepsilon - (n\pi/W_1)^2} ,$$

are the propagation constant of the structure. Taking into account the continuity and discontinuity of tangential electric and magnetic fields at (x_i^k, z_i^k), we have [16]

$$(\frac{\partial h_n^k}{\partial z} - \frac{\partial h_n^{k-1}}{\partial z})\bigg|_{z=z_i^k} = \frac{-2j\omega\mu\varepsilon}{n\pi}\sin(\frac{n\pi(x_i^k + b/2)}{b}), \quad (3a)$$

$$h_n^k(x_i^k, z_i^k) = h_n^{k-1}(x_i^k, z_i^k) . \quad (3b)$$

(a)   (b)
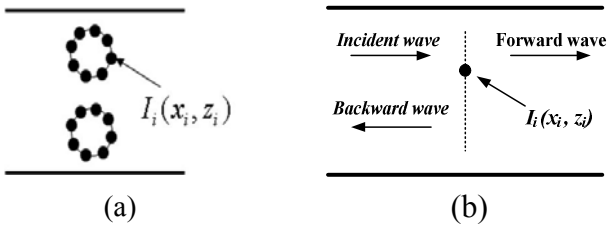
Fig. 2. (a) A pair of circular posts that are composed of a number of current delta function (b) a current delta function in the rectangular waveguide.

(a)

(b)
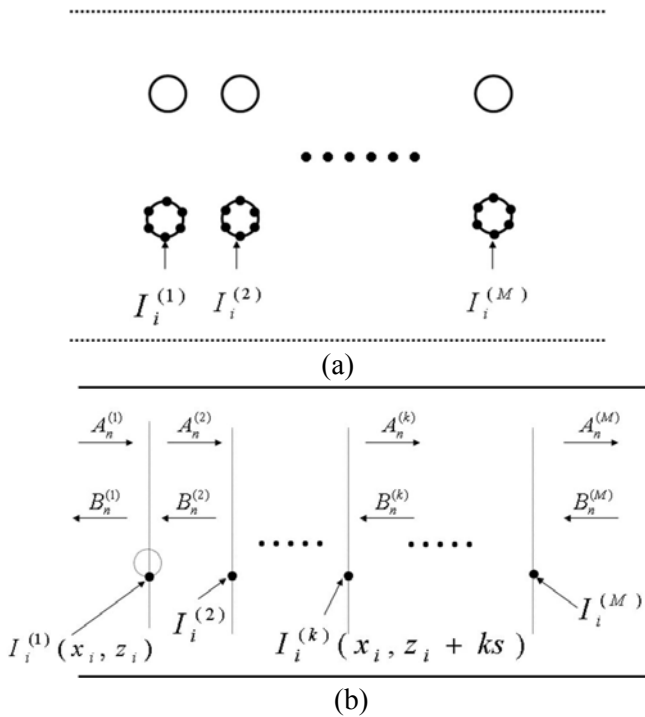
Fig. 3. (a) SIW's post pairs enclosed with lateral conducting walls (b) currents delta functions of the structure.

By inserting (2a) in (3), following two recursive equations are obtained.

$$[A^k] = [A^1] + \sum_{r=2}^{k}[C_1^r]\cdot[I^r] , \quad (4a)$$

$$[B^k] = [B^1] + \sum_{r=2}^{k}[C_2^r]\cdot[I^r], \quad (4b)$$

in which

$$[A^k] = [A_1^k, \ldots, A_N^k]^T, \quad [B^k] = [B_1^k, \ldots, B_N^k]^T$$

and $[I^r] = [I_1^r, \ldots, I_P^r]^T$.

The rth-row and s^{th}-column element of the coefficient matrices are as follows

$$\begin{cases} C_{1,rs}^k = \dfrac{\omega\mu\varepsilon}{r\pi\beta_r}\sin(\dfrac{r\pi(x_s^k + b/2)}{b})\cdot\exp(j\beta_r z_s) \\ C_{2,rs}^k = \dfrac{-\omega\mu\varepsilon}{r\pi\beta_r}\sin(\dfrac{r\pi(x_s^k + b/2)}{2})\cdot\exp(-j\beta_r z_s) \end{cases} ,$$

$$r = 1,2,\ldots,N \ and \ s = 1,2,\ldots, P^k$$

where, N and P^k are the number of modes and current filaments in region k, respectively. The other sets of equations are achieved by matching the tangential electric and magnetic fields at the junctions of input and output waveguide ports to SIW region. By applying mode matching technique at $z=0$ and $z=L$, the following equations are extracted as [17]

$$[E^1][A^1] + [E^2][B^1] = [E_{Exc}] . \quad (5a)$$

$$[F^1][A^M] + [F^2][B^M] = [0] . \quad (5b)$$

where,

$$E_{rs}^1 = \sum_{n=1}^{N}(\frac{2\beta_s s\pi f(r,n) f(s,n)}{W_1 b\beta_n^*}) + (r\pi/2)\delta_{rs} ,$$

$$E_{rs}^2 = \sum_{n=1}^{N}(\frac{-2\beta_s s\pi f(r,n) f(s,n)}{W_1 b\beta_n^*}) + (r\pi/2)\delta_{rs} ,$$

$$F_{rs}^1 = \left[\sum_{n=1}^{N}(\frac{-2\beta_s r\pi f(r,n) f(s,n)}{W_1 b\beta_n^*}) + (r\pi/2)\delta_{rs}\right]$$
$$exp(-j\beta_r L),$$

$$F_{rs}^2 = \left[\sum_{n=1}^{N}(\frac{2\beta_s r\pi f(r,n) f(s,n)}{W_1 b\beta_n^*}) + (r\pi/2)\delta_{rs}\right]$$
$$exp(-j\beta_r L),$$

$$E_{Exc} = 2\pi f(s,1)/W_1 ,$$

$$f(r,n) = \int_{-W_1/2}^{+W_1/2} sin(\frac{n\pi(x+W_1/2)}{W_1})$$

$$\times sin(\frac{r\pi(x+b/2)}{b})dx,$$

$$\delta_{rs} = \begin{cases} 1 & r = s \\ 0 & r \neq s \end{cases}.$$

Considering (4) and (5) for k=M, the following relations are obtained.

$$[A^1] = [U_1][E_{Exc}] + \sum_{r=2}[V_1^r][I^r], \qquad (6a)$$

$$[B^1] = [U_2][E_{Exc}] + \sum_{r=2}[V_2^r][I^r]. \qquad (6b)$$

In which [U] is the unit matrix and

$$[U_1] = -[G_1]^{-1}[F_2][E_2]^{-1},$$

$$[V_1^r] = -[G_1]^{-1}([F_1][C_1^r] + [F_2][C_2^r]),$$

$$[U_2] = -[E_2]^{-1}([U] + [E_1][G_1]^{-1}[F_2][E_2]^{-1}),$$

$$[V_2^r] = -[E_2]^{-1}[E_1][G_1]^{-1}([F_1][C_1^r] + [F_2][C_2^r]),$$

$$[G_1] = [F_1] - [F_2][E_2]^{-1}[E_1].$$

Hence, using (4) and (6), $[A^k]$ and $[B^k]$ can be written in terms of excitation wave and currents on posts. This allows us to apply Galerkin's testing procedure into the solution process. Equating the total tangential electric field to zero at the points of the filaments results in $\sum_{k=2}^{M}P^k$ equations and $\sum_{k=2}^{M}P^k$ unknowns as

$$\sum(-n\pi/b)\sin(n\pi(x_p^k + b/2)) \times$$
$$(A_n^k \exp(-j\beta_n^k z_p^k) + B_n^k \exp(j\beta_n^k z_p^k)) = 0 \qquad (7)$$

In which (x_p^k, z_p^k) indicates the location of pth-current filament in k^{th}-region and $k \in \{1, 2, \ldots, M\}$. By inserting (4) in (7), the coefficients of currents on posts and field distribution in the structure can be achieved. Scattering parameters at waveguide ports are obtained from following relations

$$[S_{11}] = [B^0] = [E] - [H_1][A^1 - B^1], \qquad (8a)$$

$$[S_{21}] = [A^{M+1}] = [H_2][A^M] - [H_3][B^M]. \qquad (8b)$$

In which the elements of the above matrices are as follows

$$H_{1,rs} = \frac{2s\beta_s f(r,s)}{rW_1 b\beta_r^*},$$

$$H_{2,rs} = \frac{2s\beta_s f(r,s)}{rW_1 b\beta_r^*}\exp(-j\beta_s L),$$

$$H_{3,rs} = \frac{-2s\beta_s f(r,s)}{rW_1 b\beta_r^*}\exp(j\beta_s L),$$

and E is a $1 \times N$-columnar vector which depends on the excitation mode of the input waveguide port. Considering the TE_{n0}- mode as an excitation mode, the nth element of R is 1 and the other elements are zero.

In the above formulation, W_1 is the equivalent width of SIW which should result in minimum reflection when these two waveguide ports are located at input and output of SIW waveguide, according to Fig. 1. In this case, W_1 is chosen as an unknown parameter. Optimization process initiates with $W_1 = W$ and by reducing the value of W_1 in each step, the value of which results in minimum reflection is considered as an equivalent width of SIW.

B. Discontinuity along the propagation direction

By obtaining the equivalent waveguide width of the SIW, it is possible to evaluate the above procedure for the analysis of the longitudinal discontinuity along the substrate integrated waveguide. Figure 4 shows an inductive discontinuity in the SIW structure. In this case, in addition to SIW's posts, the inductive post is divided into a number of current filaments. Following the above procedure, the currents on posts and the scattering parameters of the discontinuity can be calculated from (7) and (8).

III. RESULTS AND VALIDATION EXAMPLES

It is shown, in the following, that the presented technique provides good agreement with recently theoretical and measurement data. Consequently, the proposed method is applied to the analysis of microwave and millimeter-wave SIW circuits. As a first case, consider the structure shown in Fig. 1 with the geometrical parameters of $d = 0.8\,mm$, $S = 2\,mm$, $W = 7.2\,mm$, $b=10\,mm$, and $\varepsilon_r = 2.33$. Equivalent waveguide width is an important parameter of the SIW structure and depends

strongly on post diameter (d), distance between cross-sectional (W) and longitudinal (S) posts [6]. Equivalent width results in minimum reflection at z=0 and has distinctly been denoted by W_1 in Fig. 1. The reflection coefficient of the structure as a function of port width W_1, is indicated in Table 1. As it shows, increasing the number of posts in the longitudinal direction caused decreasing the effect of coupling between input/output posts with walls at *z=0* and *z=L.* As a result, the equivalent width inclined to an optimum value. This value is in good accuracy in comparison to the result of W_{eff}=6.866 *mm* obtained from the closed-form formulas of [6, 7].

As the result shows, since the equivalent width of SIW is very near to its physical width, optimization process is not time consuming and after two or three steps, the method is converged. This effective width is very vital in SIW applications especially in filter designs. Dispersion characteristic diagram of SIW as a function of frequency compared with that of a rectangular waveguide whose equivalent width is calculated from [6] is illustrated in Fig. 4. The comparison verifies the accuracy of the proposed method. Furthermore, the electric field in SIW at a region between posts is illustrated in Fig. 5. As expected, outside of posts electric field diminishes exponentially. This guarantees the above mentioned point as the distance between posts is very small in comparison to wavelength in the structure, the leakage of the electromagnetic fields is negligible and the structure acts as a waveguide.

The second example consists of an inductive post discontinuity in the SIW structure, as shown in Fig. 6, with the following parameters: *d=1.1 mm, S=2 mm, W=7.2 mm, and* $\varepsilon_r = 2.33$. The parameters of lumped equivalent circuit of discontinuity are necessary to design a bandpass filter.

The variation of inductance as a function of post offset from center line of the structure is shown in Fig. 6. As the parameter *e* increased, the inductance of the circuit decreased which results in more reflection.
An important feature of the method of analysis is that the fields and currents in the structure can be easily monitored. As an example, current density on posts as a function of post angle for e=2 mm is shown in Fig. 7.

Following the filter design procedure and using the equivalent circuit parameter in Fig. 6, a third order bandpass filter is designed and analyzed by applying the mentioned method. Our simulation result is compared to the results from FDTD method and measurement of [10] is shown in Fig. 8. Good agreement between the results verifies the accuracy of the method.

As a last example, a third order bandpass post filter consisting of cylindrical cavities coupled to rectangular cavity through inserted posts, reported in [18], is analyzed. The configuration of the filter is shown in Fig. 9.

Table 1: S_{11}(dB) in terms of number of post pairs, for various values of W_1 at f=15 GHz for P^k=12

	W_1 =6.6 mm	W_1 =6.7 mm	W_1=6.8 mm	W_1=6.9 mm
M=2	-24	-33	-35	-24
M=3	-20	-26	-43	-25.4
M=4	-19.6	-24	-32	-26
M=5	-20.2	-25	-30	-27.5
M=6	-20.6	-24.5	-33	-26.3
M=8	-20.5	-24.1	-32.7	-26
M=10	-20.6	-24.2	-32.5	-26.5
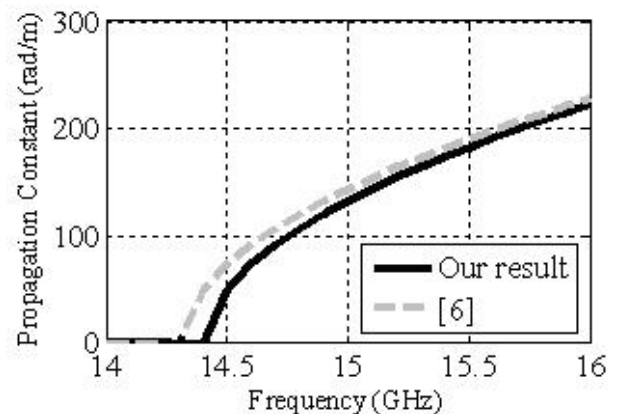
Fig. 4. Dispersion characteristic of TE_{10}-mode in the SIW.

In this case, the proposed method is accompanied by the general scattering matrix (GSM) method [19] to accelerate the speed of process. The scattering parameters of the filter, as shown in Fig. 9, are compared with those calculated with the commercial code HFSS.

With the hybrid method, the typical

computation time of the post filter in Fig. 10 is about 7 min, while the CPU time for HFSS simulation is usually over 12 min by the step size of 100 MHz. Also, the memory requirement in HFSS is much more than the proposed technique.
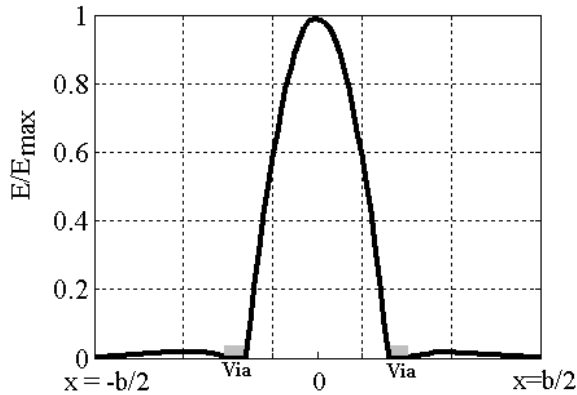
Fig. 5. Ratio of electric field to maximum value of incident electric field at the region between gaps.
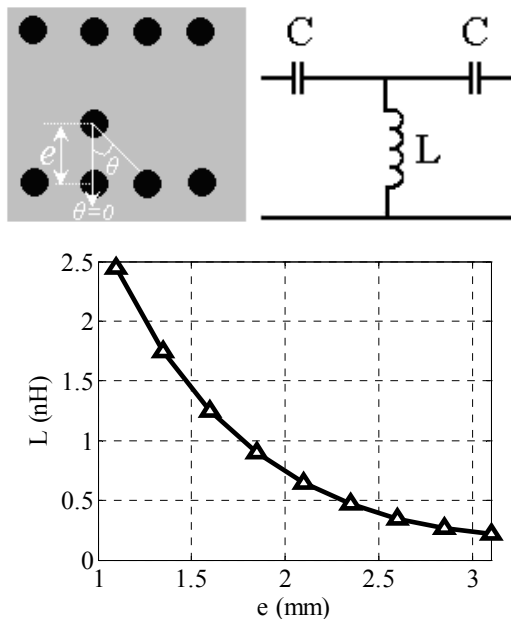
Fig. 6. Variation of inductance of equivalent circuit versus post distance e, from the waveguide side walls.
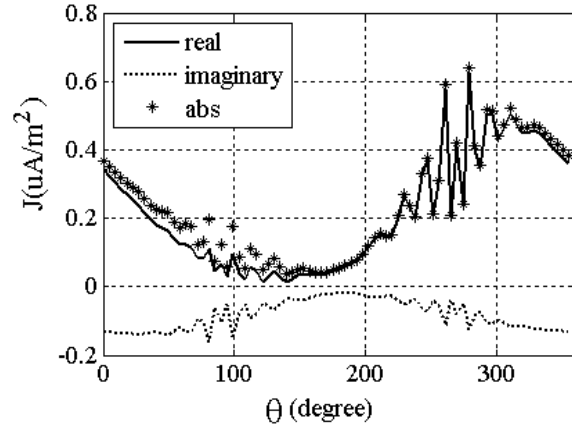
Fig. 7. Current density versus angle from center of the inductive post for e=2 mm.
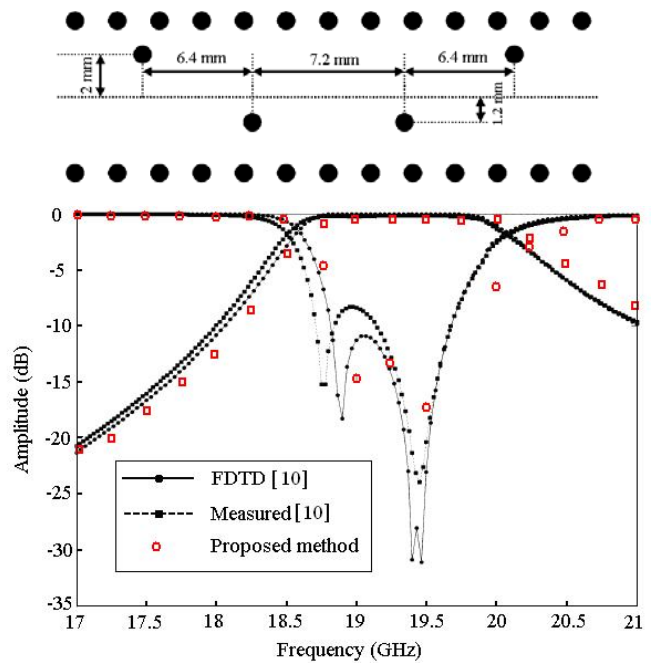
Fig. 8. Measured and simulated scattering parameters of the inductive post filter.

VI. CONCLUSION

A hybrid approach which combines the method of moment and mode matching technique was proposed to study substrate integrated waveguide circuits with longitudinal discontinuities. In comparison to other numerical techniques, the proposed method is based on field theory and gives more insight about the electromagnetic behavior of the structure. Inserting waveguide ports in input and output of SIW permits to extract equivalent waveguide

width Also, the proposed method is validated through some examples. It provides excellent agreement with measurement and theoretical results reported in recent literatures and commercial electromagnetic simulators. Also, field distributions and current density on posts as well as dispersion properties of the SIW structure are investigated. It confirms that the SIW has most properties of conventional waveguide and is a very good candidate for designing microwave circuits.
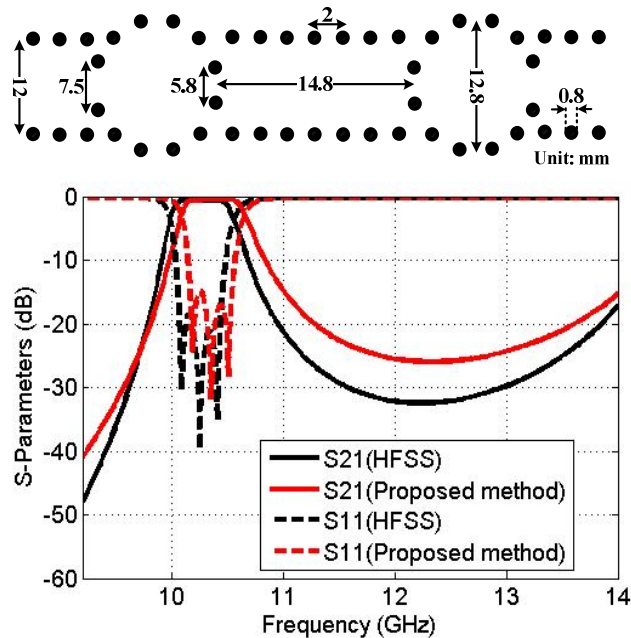
Fig. 9. Simulated scattering parameter of the bandpass post filter.

REFERENCES

[1] M. Abdolhamidi and M. Shahabadi, "X-Band Substrate Integrated Waveguide Amplifier," *IEEE microwave and wireless components letters,* vol. 18, pp. 815-817, 2008.

[2] S. Lin, S. Yang, A. E. Fathy, and A. Elsherbini, "Development of a Novel UWB Vivaldi Antenna Array using SIW Technology," *Progress In Electromagnetics Research*, vol. 90, pp. 369–384, 2009.

[3] M. Salehi, E. Mehrshahi, and R. Rezaeisarlak, "Stopband Improvement of Substrate Integrated Waveguide Filters Using Slotted Ground Structures," *Asia-Pacific Microwave Conference (APMC)*, pp. 1717-1719, 2010.

[4] F. Giuppi, A. Georgiadis, M. Bozzi, S. Via, A. Collado, and L. Perregrini, "Hybrid Electromagnetic and Non-Linear Modeling and Design of SIW Cavity-Backed Active Antennas," *The Applied Computational Electromagnetics Society (ACES)Journal* vol. 25, pp. 682 – 689, Aug. 2010.

[5] Y. Cassivi, L. Perregrini, P. Arcioni, M. Bressan, K. Wu, and G. Conciauvo, "Dispersion Characteristics of Substrate Integrated Rectangular Waveguide," *IEEE Microwave and Wireless Components Letters,* vol. 12, pp. 333-335, 2002.

[6] F. Xu and K. Wu, "Guided-Wave and Leakage Characteristics of Substrate Integrated Waveguide," *IEEE Transactions on microwave theory and techniques,* vol. 53, 2005.

[7] M. Salehi and E. Mehrshahi, "A Closed-Form Formula for Dispersion Characteristics of Fundamental SIW Mode," *IEEE Microwave and Wireless Components Letters,* vol. 21, pp. 4-6, Jan. 2011.

[8] C. H. Tseng and T. H. Chu, "Measurement of Frequency-Dependent Equivalent Width of Substrate Integrated Waveguide," *IEEE Transactions on Microwave Theory and Techniques,* vol. 54, p. 1431, 2006.

[9] F. Xu, Y. Zhang, W. Hong, K. Wu, and T. J. Cui, "Finite-Difference Frequency-Domain Algorithm for Modeling Guided-Wave Properties of Substrate Integrated Waveguide," *IEEE Transactions on Microwave Theory and Techniques,* vol. 51, pp. 2221-2227, 2003.

[10] F. Xu, K. Wu, and W. Hong, "Domain Decomposition FDTD Algorithm Combined with Numerical TL Calibration Technique and its Application in Parameter Extraction of Substrate Integrated Circuits," *IEEE Transactions on Microwave Theory and Techniques,* vol. 54, p. 329, 2006.

[11] L. Yan and W. Hong, "Investigations on the Propagation Characteristics of the Substrate Integrated Waveguide Based on the Method of Lines," *IEE Proceedings on Microwaves, Antennas and Propagation,* vol. 152, pp. 35-42, 2005.

[12] E. Arnieri and G. Amendola, "Analysis of Substrate Integrated Waveguide Structures Based on the Parallel-Plate Waveguide

Green's Function," *IEEE Transactions on Microwave Theory and Techniques,* vol. 56, pp. 1615-1623, 2008.

[13] E. Arnieri and G. Amendola, "Method of Moments Analysis of Slotted Substrate Integrated Waveguide Arrays," *IEEE Transactions on Antennas and Propagation,* vol. 59, pp. 1148-1154, 2011.

[14] E. Mehrshahi and M. Salehi, "A Simple Technique for Propagation Characteristics of Substrate Integrated Waveguide," *The Applied Computational Electromagnetics Society (ACES) Journal* vol. 25, pp. 690-695, Aug. 2010.

[15] R. Rezaeisarlak, E. Mehrshahi, and H. R. Sadreazami, "Hybrid of Moment Method and Mode Matching Technique to Study Substrate Integrated Waveguide," in *International Conference on Microwave and Millimeter Wave Technology (ICMMT),* 2010, pp. 1980-1982.

[16] R. E. Collin, *Field theory of guided waves*: IEEE press New York, 1991.

[17] D. M. Pozar, "Microwave Engineering, 3rd," ed: John Wiley & Sons, Hoboken, NJ, USA, 2005.

[18] E. Mehrshahi, M. Salehi, and R. Rezaeisarlak, "Substrate Integrated Waveguide Filters with Stopband Performance Improvement," in *International Conference on Microwave and Millimeter Wave Technology (ICMMT)*, pp. 2018-2020, 2010.

[19] T. Itoh, *Numerical techniques for microwave and millimeter-wave passive structures*: John Wiley & Sons, New York, 1989.

Reza Rezaiesarlak was born in Aligoodarz, Iran. He received the B. Sc. degree from Shahid Beheshti University (SBU), Tehran, Iran, and the M.Sc. degree, in Electrical Engineering, from Iran University of Science and Technology (IUST), Tehran, in 2004 and 2007, respectively. From 2007, he has worked on various microwave projects including active and passive microwave circuits.

His current research interests include numerical techniques in electromagnetics, applied mathematics, and optimum design of microwave filters and antennas.

Mehdi Salehi was born in Isfahan, Iran, in 1979. He received the B.Sc. degree from Isfahan University of Technology (IUT), Iran, in 2001, and M.Sc. degree from Malek Ashtar Uniuverity of Technology (MUT), Tehran, Iran, in 2006 both in Electrical Engineering. He is currently working toward his Ph.D. degree in Electrical Engineering at Shahid Beheshti University (SBU), Tehran, Iran.

He worked as a researcher in Information and Communication Technology Institute (ICTI) on RF circuit design from 2001 to 2003. His current research interests include numerical methods in electromagnetic and advanced microwave and millimeter-wave circuits and components.

Esfandiar Mehrshahi was born in Tehran, Iran, in 1964. He received the B.Sc. degree from the Iran University of Science and Technology, Tehran, Iran, in 1987, and the M.Sc. and Ph.D. degrees from the Sharif University of Technology, Tehran, Iran, in 1991 and 1998, respectively, all in Electrical Engineering. Since 1990, he has been involved in several research and engineering projects at the Iran Telecommunications Research Center (ITRC).

He is currently an Assistant Professor at Shahid Beheshti University (SBU), Tehran, Iran. His main areas of interest are the nonlinear simulation of microwave circuits, low phase noise oscillators, and computational electromagnetics.